Local-Illuminated Ultrathin Silicon Nanomembranes with Photovoltaic Effect and Negative Transconductance

By *Ping Feng, Ingolf Mönch, Gaoshan Huang, Stefan Harazim, Elliot J. Smith, Yongfeng Mei,** and *Oliver G. Schmidt*

Inorganic nanomembranes as a versatile class of building blocks in nanoscience and nanotechnology[1–3] are attracting significant attention for many potential applications including flexible electronics,[4,5] metamaterials,[6,7] strained silicon technology,[8,9] and bioanalytic microsystems.[10,11] Schottky barriers at contacts to nanomaterials are often observed and may play a critical role for their electrical properties,[12–14] in particular for nanomembranes.[15] On the other hand, certain tricks played on Schottky barriers can offer routes to novel devices like ambipolar transistors[16] and solar cells.[17,18] Recently, local illumination was exploited in scanning photocurrent spectroscopy to probe the effect of contact properties on device characteristics of silicon nanowires, graphene, and carbon nanotubes.[14,19–21] However, there are only few reports to apply such basic Schottky contacts to nanomaterials to realize interesting electronic devices.[18]

Here, we demonstrate that ultrathin silicon nanomembranes (SiNMs) on insulators under local illumination reveal a gate-controlled photovoltaic effect and negative transconductance in Schottky transistors applying both homo- and heterocontacts. Tiny variations of Schottky barriers between source and drain contacts are responsible for the photovoltaic effect in ultrathin SiNMs and can be enhanced by the gate voltage and/or contact design. Such a photovoltaic effect induces a built-in voltage and thus leads to a steep increase of the current across the channel, which is manifested in a so-called negative transconductance.

A test transistor based on SiNMs under local laser illumination is schematically shown in **Figure 1a**, where the Si substrate serves as a back gate. The source and drain electrodes are contacted with different (Ti and Cr/Au) or the same (Cr/Au and Cr/Au) metals, thus creating hetero- or homocontacts for electrical investigations. Figure 1b and c show the current (I_{SD}, source-drain current) versus gate voltage (V_G) curves of 27 nm SiNM-based devices at a fixed drain voltage (V_D) of –0.1 V for hetero- and homocontacts. The ambipolar characteristics, when the laser is off, indicate that both devices are Schottky barrier transistors. Negative gate voltages result in hole accumulation in the channel and a *p*-type operation mode, whereas positive gate voltages lead to electron accumulation and an n-type operation mode.[15] When a focused laser spot illuminates the middle region of the SiNM channel, unusual I_{SD}–V_G curves

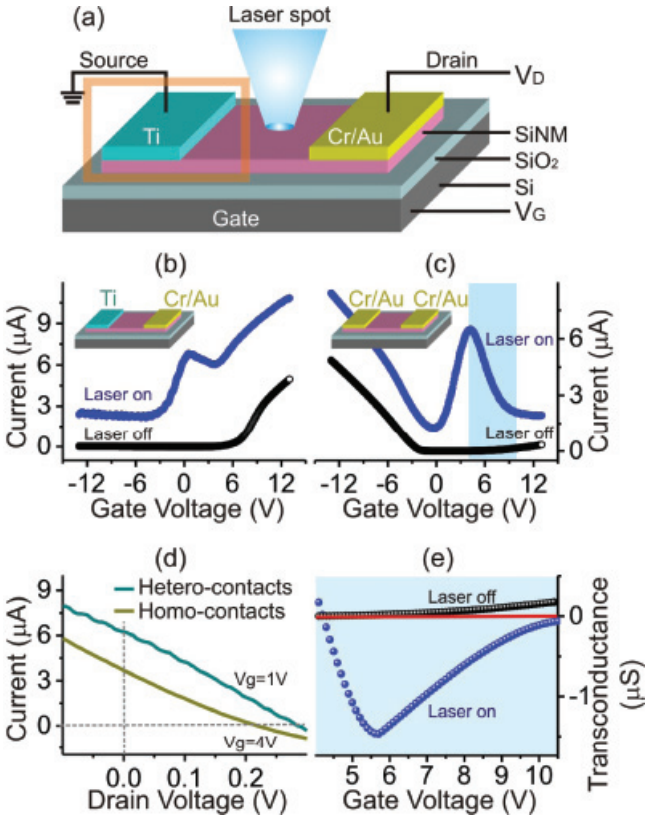

Figure 1. a) Schematic of the SiNM devices and the measurement principle. The voltages applied to the drain and gate electrodes can be changed. A laser spot with controlled power and position, illuminates the SiNM channel. I_{SD}–V_G results obtained from b) heterocontacts with Ti and Cr/Au and c) homocontacts with Cr/Au and Cr/Au when the laser is on and off. When the laser is off, the device exhibits ambipolar characteristics, with increasing the positive gate voltage, the current increases gradually; in contrast, when the laser is on, with increasing positive gate voltage, the current increases quickly to a high level, and then decreases before rising again in a moderate fashion. d) I_{SD}–V_D curves for SiNMs (with hetero- and homocontacts) illuminated in the middle by a laser power of 400 μW. Gate voltages are 4V and 1V, respectively. e) Transconductance deduced from the shadow region in c. The thickness of the SiNM used here is 27 nm, the length and width of the SiNM channel are 12 and 20 μm, respectively, and V_D = –0.1 V.

[*] Dr. P. Feng, Dr. I. Mönch, Dr. G. Huang, S. Harazim, E. J. Smith, Dr. Y. F. Mei, Prof. O. G. Schmidt
Institute for Integrative Nanosciences
IFW Dresden
Helmholtzstr. 20, D-01069 Dresden (Germany)
E-mail: y.mei@ifw-dresden.de
Dr. Y. F. Mei
Department of Materials Science
Fudan University
Handan Road 220, 200433 Shanghai (China)

DOI: 10.1002/adma.201000583

are measured; with increasing positive gate voltage, the current increases quickly to a high level, then decreases before rising again in a moderate fashion. Interestingly, for gate voltages at maximum I_{SD}, a pronounced photovoltaic effect is observed in both devices as shown in Figure 1d, where V_G = 1 V for heterocontacts and V_G = 4 V for homocontacts. We estimate the total efficiency of our gate-controlled photovoltaic devices in the range of 0.05% and the quantum efficiency at around 2%.

In a transistor, the transconductance is defined as the derivative of the current across the channel over the gate voltage.[22] Normally, the conductance changes monotonically with the gate voltage and leads to a positive transconductance. In contrast, a negative transconductance can be achieved with double- or grating-gated transistors.[23,24] In our local-illuminated SiNM-based transistor, a negative transconductance is observed in the shadow region of Figure 1c and occurs for gate voltages between 4 V and 11 V (see Figure 1e).

Such unusual I_{SD}–V_G results responsible for the negative transconductance can be modulated by the laser power and the drain voltage, as shown in Supporting Information (S-)Figure 1a and b, respectively. We take the homocontacted case as an example from Figure 1c. With decreasing laser power from 100% to 0.5% of the full power at V_D = –0.1 V, the current near V_G = 4.2 V decreases substantially and can be ascribed to the decrease of photogenerated carrier densities as shown in S-Figure 1a. By changing the drain voltage from –0.1 to –0.9 V (under full laser power illumination), the current across the channel increases and is due to a faster transport of carriers at a higher bias. An important feature to note is that even for V_D = 0 V, finite current still flows in the channel, as shown in the bottom curve of S-Figure 1b. This directly confirms the photovoltaic effect present in the device.

For V_D = 0 V, as clearly shown in the I_{SD}–V_G curve in **Figure 2a**, four features are revealed: 1) the gate voltage can modulate the current inversely, 2) the maximum current can be several microamperes, 3) the current is negative at large V_G and approaches –1 μA for V_G = 20 V, and 4) around the peak the source-drain current is positive which means that photogenerated holes move to the drain and electrons to the source. The last feature indicates that there is a substantial built-in lateral electric field which separates excess carriers when V_G is around 4 V. We measured the I_{SD}–V_D curves at V_G = 0, 2 and 4 V, as shown in Figure 2b,c, and d, respectively, to estimate the lateral photovoltage. In each figure, results at five different laser powers are shown. The photovoltage is very low at V_G = 0 V, which increases to about 0.1 V at V_G = 2 V and is as high as 0.22 V at V_G = 4 V. The laser power mainly affects the current. These results indicate the presence of considerable photovoltages at appropriate gate voltages and that the corresponding electric fields point into the direction from source to drain.

In order to analyze the potential profiles of the device, I_{SD}–V_G curves are recorded as the laser spot is scanned from the source to the drain.[20] The laser was operated at full power and the drain voltage was set at –0.1 V. The results are shown in **Figure 3**. The color spots (labeled by numbers) in Figure 3b mark the laser spot positions and the results are shown in Figure 3a by bold lines with the same corresponding colors (or numbers). The main features of the curves are significantly affected by the position of the laser spot. When the laser spot is located near the source (as shown by the black curve at the bottom of Figure 3a) the source-drain current decreases with increasing gate voltage and changes the sign when the gate voltage is very large. It is known that the gate voltage can adjust carrier densities, leading to the change in the relative distance between the conduction/valence band edge and the Fermi level.[22] As a result, the Schottky barrier shape at the contact will be changed.[13] In this device, the barrier height for electrons at the source is lower than at the drain. At appropriate gate voltages, as shown by the middle sketch, the band bending direction at the source and drain contacts can be different. We therefore propose a schematic band diagram to explain the observed results, as shown in Figure 3c. As V_G increases, the barrier profile near the source changes significantly. At this point, local laser illumination generates many excess carriers, which are separated by the built-in electric field, thus producing the photocurrent. At large negative and positive gate voltages, the electric field has opposite directions, thus the current has opposite signs, as indicated by the black curve in Figure 3a.

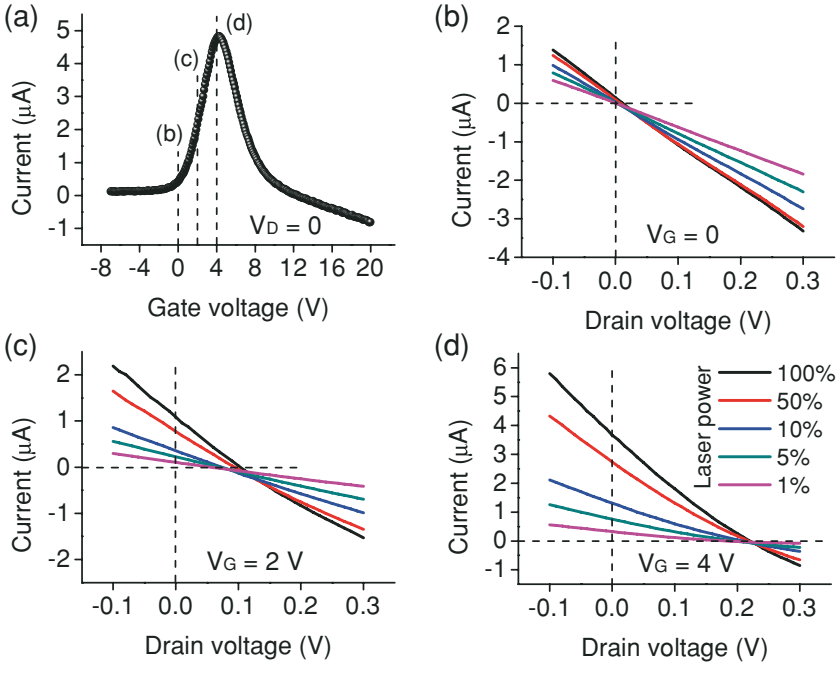

Figure 2. a) I_{SD}–V_G curve measured for a drain voltage of 0 V. A laser spot at full power illuminates the middle area of the channel. The current is strongly modulated by the gate voltage and can be several microamperes at a midlevel of V_G. At three representative V_G as marked in a, the I_{SD}–V_D results are shown in b: V_G = 0 V, in c: V_G = 2 V, and in d: V_G = 4 V. In each figure, results for five different laser powers are shown. The photovoltage is adjusted by the gate voltage, whereas the current is mainly affected by the laser power.

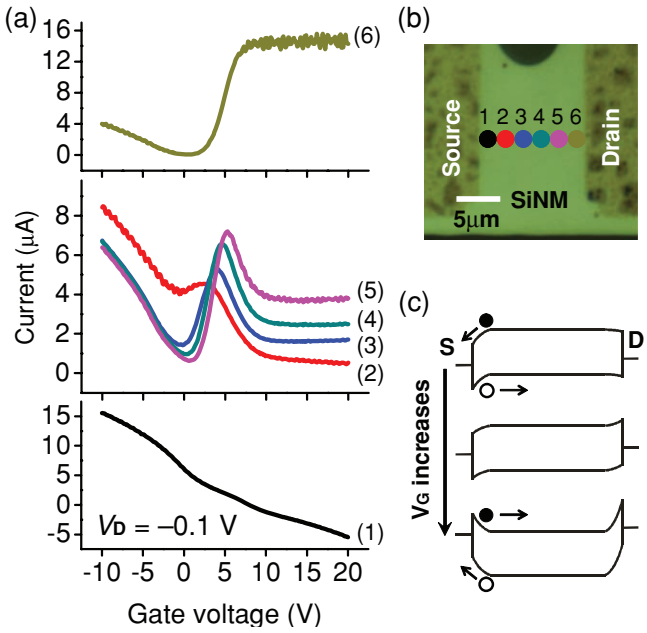

Figure 3. a) I_{SD}–V_G curves recorded as the laser spot (b) is scanned from the source to the drain. The laser power is 400 μW and the drain voltage is –0.1 V. The color in (b) defines the laser spot positions and the electrical results are shown in (a) by bold lines with the same corresponding colors. The characteristics of the curves are significantly affected by the position of the laser spot. c) Schematic band diagram to interpret the observed results; changing the gate voltage causes a shift of the conduction and valence band edge, leading to a change of the Schottky barrier profiles at the source and drain contacts. In this device, the barrier height for electrons at the source is lower than at the drain. At appropriate gate voltages, as shown by the middle sketch, the band bending direction at the source and drain contacts can be different. The solid and open circles represent electrons and holes, respectively. S labels the source and D the drain.

When the laser spot is moved to the drain, as shown in the upper panel of Figure 3a, the flowing direction of the current remains nearly unchanged due to the presence of the drain voltage, in contrast to the case when the laser spot is located near the source.

As the laser spot is scanned to the middle region of the channel, abnormal current peaks appear and the position of the peaks moves to higher gate voltages, as shown in the middle portion of Figure 3a. The appearance of the peaks indicates that at appropriate gate voltages, photogenerated carriers can be effectively separated. We have found in Figure 2 that a large voltage in the source-drain direction can be induced. It is also known that switching of the bending direction of energy levels at the contact can be induced by the gate.[25] If the barrier height for electrons at the source is lower than at the drain, such a built-in voltage will be naturally produced when the gate voltage increases to appropriate levels, where the band bends down at the source and bends up at the drain, as indicated in the middle sketch of Figure 3c. In the dark, the current is limited by the low injection of carriers at the contacts. In contrast, when the middle area of the channel is irradiated by the laser light, many carriers are generated in the SiNM and are separated by the electric field, giving rise to a large current. Further increase in the gate voltage make the bands at the source and drain bend in the same direction again, hence the current decreases, which results in the decrease of the conductance and the observed negative transconductance.

To support the above discussions, we measured the current versus bias voltage curves with a grounded source and drain without using the gate; the black and red curves in S-Figure 2a are recorded when the bias is applied to the drain and source contacts, respectively. For negative bias voltages, the injection of electrons is much easier from the source, indicating that the barrier height for electrons at the source is lower than at the drain,[26] consistent with our assumption. For positive bias, the injection of holes is much easier from the drain, which means that the barrier height for holes at the drain is lower, or the barrier height for electrons at the drain is higher than at the source.[26] In addition, we measured I_{DS} (drain-source current) versus V_G curves at different source voltages when the drain was grounded, as shown in S-Figure 2b. During the measurements, the source voltage was changed from 0 to 0.8 V and the laser light, at full power, illuminated the middle area of the channel. The barrier height for electrons at the source is lower than at the drain; therefore, the current peaks should appear when the source voltage is positive, which – indeed – is experimentally revealed in S-Figure 2b. These results are consistent with Figure 3c.

Similar results can be realized in the device fabricated from 20 nm thick SiNMs with either homo- or heterocontacts, which strongly support our interpretation. **Figure 4** shows the electrical properties for the transistor made from the 20 nm SiNM with homocontacts. The results can be well explained by considering that the barrier height for electrons at the source is higher than at the drain. Figure 4a shows the I_{DS}–V_G curves obtained in the dark (red curve) and when a laser light at full power illuminated the middle area of the channel (black curve). The drain voltage was 0.1 V. The corresponding g_m–V_G curve under laser illumination is shown in Figure 4b. An inversion of the transconductance from positive to negative can be seen at approximately V_G = 6 V. The I_{DS}–V_D curve recorded at this gate voltage indicates that the photovoltage is about –0.1 V, as shown in Figure 4c. The inset of Figure 4c is used to sketch the operation of the device when the drain voltage is 0 V. A decrease or increase of the drain voltage from 0 V will move the band edge at the drain upwards or downwards, thus leading to the decrease or increase of the circuit voltage and the final current, respectively. The current versus bias voltage curves in Figure 4d, without using the gate, indicate clearly that the barrier height for electrons at the source is higher than at the drain. Therefore, in SiNM-based Schottky barrier transistors, the effect introduced by the difference of the band bending at the source and drain contacts can be well manipulated by the gate to produce a lateral voltage. Having created this voltage, the photovoltaic effect emerges as the devices are excited by local laser illumination and causes the appearance of negative transconductance.

The negative transconductance we show here is induced by the photovoltaic effect in devices with both hetero- and homocontacts. The photovoltaic effect for heterocontacts can be easily understood by different Schottky barriers at the source and drain causing different degrees of band bending at the contacts of the

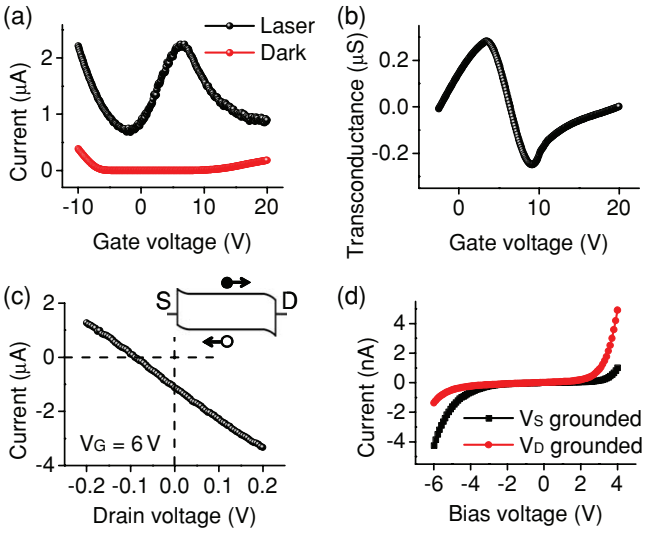

Figure 4. Negative transconductance in the device fabricated from 20 nm thick SiNMs. The length and width of the channel are approximately 12 and 14 μm, respectively. a) I_{DS}–V_G curves obtained in the dark (red curve) and when a laser spot at full power illuminates the middle area of the channel (black curve); the drain voltage is 0.1 V. b) Corresponding g_m–V_G curve under laser illumination. c) I_{DS}–V_D curve measured when the gate voltage is 6 V and the middle part of the channel is irradiated by a full power laser spot. The inset band diagram illustrates the operation of the device when the drain voltage is 0 V. The solid and open circles represent electrons and holes, respectively. S labels the source and D the drain. d) Current vs. bias voltage curves without using the gate. The black/red curve is recorded when the source/drain contact is grounded and the bias voltage is applied on the drain/source contact. Here, the barrier height for electrons at the source is higher than at the drain.

devices. However, a similar behavior is also revealed for homocontacts, which we explain by thickness and strain fluctuations in the thin top Si layer of the SOI wafers. The control of layer homogeneity is well-known as a crucial challenge in SOI technology.[27] At the metal semiconductor contact, the metal's electron wave function decays into the semiconductor, leading to the formation of a depletion layer on the semiconductor side of the interface.[28] Such an electron wave function decay is expected to be sensitive to the properties of the semiconductor. It has been reported that both Si thickness and strain substantially affect the Schottky barrier height of metal-Si contacts.[29] In our system, the SiNMs experience thickness fluctuations of roughly 10% and varying internal strains. Considering that the channel has a length of 10–20 μm (almost a thousand times longer than the channel thickness), it is reasonable to assume that the conditions, e.g. thickness fluctuations and strains of the SiNMs, at the source and drain are different, which result in different band bendings at the contacts.

In summary, we have demonstrated a gate-controlled photovoltaic effect and negative transconductance in locally illuminated ultrathin silicon nanomembranes used in Schottky transistors. Detailed measurements reveal that the observed effects originate from the difference in band bending at the source and drain contacts (even for homocontacts). Our results provide a useful method to disclose contact properties of nanomaterials and open alternative ways for novel nano-optoelectronic devices based on the photovoltaic effect.

Experimental Section

The Si nanomembranes (SiNMs) are part of silicon-on-insulator (SOI) wafers made by SOITEC Inc. Two types of wafers, with Si/SiO_2 thicknesses of 27/100 and 20/150 nm respectively, were used. The SiNMs have a boron doping level of 10^{15} cm^{-3}. To fabricate the SiNM-based thin-film transistors, we used a series of microelectronic processes, including photolithography, reactive ion etching, electron beam evaporation, thermal annealing etc. Briefly, the original SiNMs were patterned by photoresist and etched by reactive fluorine ions. Subsequently, patterns for the source and drain were defined. Ti (30 nm) or Cr/Au (2/30 nm) electrodes were realized by electron beam evaporation and liftoff. Improved electrical contacts were obtained by rapid thermal annealing in Ar at 500 °C for 3 min with a ramping rate of 16 °C/s. Each device has a SiNM channel, which is 10–20 μm in length and width, and a Si back gate, as shown in Figure 1a. A laser spot with a diameter of 2–3 μm provides local illumination. The 442 nm laser originates from a micro-Raman spectrometer system (InVia, Renishaw) and has a full power of 400 μW at the focal point. The measurements were performed by a semiconductor parameter analyzer (Agilent, 4156C) at room temperature.

Supporting Information

Supporting Information is available online from Wiley InterScience or from the author.

Acknowledgements

We thank Martin Bauer and Barbara Eichler for experimental help. P.F. is grateful to the Alexander von Humboldt Foundation for fellowship support. This work was financially supported by a Grant from a Multidisciplinary University Research Initiative (MURI) sponsored by the U. S. Air Force Office of Scientific Research (AFOSR) Grant No. FA9550-09-1-0550.

Received: February 15, 2010
Revised: April 6, 2010
Published online: June 29,2010

[1] O. G. Schmidt, K. Eberl, *Nature* **2001**, *410*, 168.
[2] A. Cho, *Science* **2006**, *313*, 164.
[3] D.-H. Kim, J. A. Rogers, *ACS Nano* **2009**, *3*, 498.
[4] W. M. Choi, J. Song, D.-Y. Khang, H. Jiang, Y. Y. Huang, J. A. Rogers, *Nano Lett.* **2007**, *7*, 1655.
[5] A. J. Baca, J.-H. Ahn, Y. Sun, M. A. Meitl, E. Menard, H.-S. Kim, W. M. Choi, D.-H. Kim, Y. Huang, J. A. Rogers, *Angew. Chem. Int. Ed.* **2008**, *47*, 5524.
[6] S. Schwaiger, M. Bröll, A. Krohn, A. Stemmann, C. Heyn, Y. Stark, D. Stickler, D. Heitmann, S. Mendach, *Phys. Rev. Lett.* **2009**, *102*, 163903.
[7] E. J. Smith, Z. Liu, Y. F. Mei, O. G. Schmidt, *Nano Lett.* **2010**, *10*, 1.
[8] M. M. Roberts, L. J. Klein, D. E. Savage, K. A. Slinker, M. Friesen, G. Celler, M. A. Eriksson, M. G. Lagally, *Nat. Mater.* **2006**, *5*, 388.
[9] S. A. Scott, M. G. Lagally, *J. Phys. D: Appl. Phys.* **2007**, *40*, R75.
[10] Y. F. Mei, G. S. Huang, A. A. Solovev, E. Bermúdez Ureña, I. Moench, F. Ding, T. Reindl, R. K. Y. Fu, P. K. Chu, O. G. Schmidt, *Adv. Mater.* **2008**, *20*, 4085.
[11] G. S. Huang, Y. F. Mei, D. J. Thurmer, E. Coric, O. G. Schmidt, *Lab Chip* **2009**, *9*, 263.
[12] M. Freitag, M. Radosavljevic, Y. Zhou, A. T. Johnson, W. F. Smith, *Appl. Phys. Lett.* **2001**, *79*, 3326.
[13] S. Heinze, J. Tersoff, R. Martel, V. Derycke, J. Sppenzeller, Ph. Avouris, *Phys. Rev. Lett.* **2002**, *89*, 106801.

[14] Y. Ahn, J. Dunning, J. Park, *Nano Lett.* **2005**, *5*, 1367.
[15] P. Feng, I. Mönch, S. Harazim, G. S. Huang, Y. F. Mei, O. G. Schmidt, *Nano Lett.* **2009**, *9*, 3453.
[16] H.-C. Lin, K.-L. Yeh, T.-Y. Huang, R.-R. Huang, S. M. Sze, *IEEE Trans. Electron. Dev.* **2002**, *49*, 264.
[17] a) J. M. Luther, M. Law, M. C. Beard, Q. Song, M. O. Reese, R. J. Ellingson, A. J. Nozik, *Nano Lett.* **2008**, *8*, 3488; b) J. Tang, X. Wang, L. Brzozowski, D. A. R. Barkhouse, R. Debnath, L. Levina, E. H. Sargent, *Adv. Mater.* **2010**, DOI: 10.1002/adma.200903240.
[18] C. Chen, Y. Lu, E. S. Kong, Y. Zhang, S.-T. Lee, *Small* **2008**, *4*, 1313.
[19] C. Yang, C. J. Barrelet, F. Capasso, C. M. Lieber, *Nano Lett.* **2006**, *6*, 2929.
[20] E. J. H. Lee, K. Balasubramanian, R. T. Weitz, M. Burghard, K. Kern, *Nat. Nanotechnol.* **2008**, *3*, 486.
[21] N. M. Gabor, Z. Zhong, K. Bosnick, J. Park, P. L. McEuen, *Science* **2009**, *325*, 1367.
[22] S. M. Sze, *Semiconductor Devices: Physics and Technology*; Wiley, New York, **2002**.
[23] K. Ismail, W. Chu, D. A. Antoniadis, H. I. Smith, *Appl. Phys. Lett.* **1988**, *52*, 1071.
[24] A. Zaslavsky, S. Soliveres, C. Le Royer, S. Cristoloveanu, L. Clavelier, S. Deleonibus, *Appl. Phys. Lett.* **2007**, *91*, 183511.
[25] M. Freitag, J. C. Tsang, A. Bol, D. Yuan, J. Liu, Ph. Avouris, *Nano Lett.* **2007**, *7*, 2037.
[26] J. Appenzeller, M. Radosavljević, J. Knoch, Ph. Avouris, *Phys. Rev. Lett.* **2004**, *92*, 048301.
[27] G. K. Celler, S. Cristolovreanu, *J. App. Phys.* **2003**, *93*, 4955.
[28] W. Mönch, *Rep. Prog. Phys.* **1990**, *53*, 221.
[29] D. Connelly, P. J. Clifton, *J. Appl. Phys.* **2008**, *103*, 074506.